Journal of Thermal Analysis and Calorimetry, Vol. 83 (2006) 1, 213–218

THERMAL DECOMPOSITION OF HYDRONIUM JAROSITE $(H_3O)Fe_3(SO_4)_2(OH)_6$

*Ray L. Frost**, *Rachael-Anne Wills, J. Theo Kloprogge and Wayde N. Martens*

Inorganic Materials Research Program, School of Physical and Chemical Sciences, Queensland University of Technology
GPO Box 2434, Brisbane Queensland 4001, Australia

Thermogravimetry combined with mass spectrometry has been used to study the thermal decomposition of a synthetic hydronium jarosite. Five mass loss steps are observed at 262, 294, 385, 557 and 619°C. The mass loss step at 557°C is sharp and marks a sharp loss of sulphate as SO_3 from the hydronium jarosite. Mass spectrometry through evolved gases confirms the first three mass loss steps to dehydroxylation, the fourth to a mass loss of the hydrated proton and a sulphate and the final step to the loss of the remaining sulphate. Changes in the molecular structure of the hydronium jarosite were followed by infrared emission spectroscopy. This technique allows the infrared spectrum at the elevated temperatures to be obtained. Infrared emission spectroscopy confirms the dehydroxylation has taken place by 400 and the sulphate loss by 650°C. Jarosites are a group of minerals formed in evaporite deposits and form a component of the efflorescence. The minerals can function as cation and heavy metal collectors. Hydronium jarosite has the potential to act as a cation collector by the replacement of the proton with a heavy metal cation.

Keywords: *dehydration, dehydroxylation, high-resolution thermogravimetric analysis, hydronium jarosite, infrared emission spectroscopy, jarosite*

Introduction

Jarosite was first discovered on Earth in 1852 in ravines in the mountainous coast of southeastern Spain. Jarosites were discovered on Mars in 2005. Jarosites occur in the oxidized zones of sulphide minerals as a secondary mineral. Hydronium jarosite has been found at the Golden Dewdrop mine, Outalpa Station, Olary Province, South Australia. Hydronium jarosite was determined through the chemical analyses of many jarosites [1, 2]. The mineral forms a continuous series with jarosite and natrojarosite. The positive identification of the mineral was achieved through the use of NMR [3]. The mineral is typically ocherous, amber to dark brown granular masses or crystalline crusts. The formation of the mineral is not rare since concentrated acid containing solutions are common. The acidity must originate from the formation of sulphuric acid through the oxidation of sulphide deposits [4]. It has been shown that thiobacillus ferrooxidans acts as a catalyst in the formation of jarosite and hydronium jarosite [5]. The importance of jarosite formation and its decomposition depends upon its presence in soils, sediments and evaporite deposits [6]. The presence of bacteria such as thiobacillus ferrooxidans contribute to both jarosite and hydronium jarosite formation. These types of deposits have formed in acid soils where the pH is less than pH 3.0 [7]. Such acidification results from the oxidation of pyrite which may be from bacterial action or through air-oxidation.

The thermal decomposition of jarosites has been studied for considerable time [8–12]. Some studies of the thermal decomposition of hydronium jarosite have been undertaken [13, 14]. These studies are limited and do not define the decomposition of the hydronium jarosite. There have also been many studies on related minerals such as the Fe(II) and Fe(III) sulphate minerals [15–20]. Interest in such minerals and their thermal stability rests with the possible identification of these minerals and dehydrated paragenetically related minerals on planets and on Mars. The existence of these minerals on Mars would give a positive indication of the existence or at least pre-existence of water on Mars. Further such minerals are formed through crystallisation from solutions. Whether or not hydronium jarosite is found in such environments is unknown. However it is highly likely that hydronium jarosite will be found. It has been stated that the thermal decomposition of jarosite begins at 400°C with the loss of water [21]. The process is apparently kinetically driven. Water loss can occur at low temperatures over extended periods of time [21]. It is probable that in nature low temperature environments would result in the decomposition of hydronium jarosite. Recently thermogravimetric analysis has been applied to some complex mineral systems and it is considered that TG-MS analyses may also be applicable to the jarosite minerals [22–27].

* Author for correspondence: r.frost@qut.edu.au

1388–6150/$20.00

Akadémiai Kiadó, Budapest, Hungary
Springer, Dordrecht, The Netherlands

In this work we report the thermal decomposition of a synthetic hydronium jarosite using thermogravimetry and infrared emission spectroscopy.

Experimental

Minerals

To prepare pure hydronium jarosite, 4 g of $Fe_2(SO_4)_3$ was dissolved in 40 mL of water. This solution was heated at 120°C for 21 h in an autoclave, forming a golden brown precipitate. The precipitate was collected and dried under vacuum. 0.56 g of dry hydronium jarosite was obtained.

Thermal analysis

Thermal decomposition of the hydronium jarosite was carried out in a TA® Instrument incorporated high-resolution thermogravimetric analyzer (series Q500) in a flowing nitrogen atmosphere (80 cm^3 min^{-1}). 34.4 mg of sample underwent thermal analysis, with a heating rate of 5°C min^{-1}, resolution of 6, to 1000°C. With the quasi-isothermal, quasi-isobaric heating program of the instrument the furnace temperature was regulated precisely to provide a uniform rate of decomposition in the main decomposition stage. The TG instrument was coupled to a Balzers (Pfeiffer) mass spectrometer for gas analysis. Only water vapour, sulphur dioxide, sulphur trioxide, carbon dioxide and oxygen were analyzed.

Infrared emission spectroscopy

FTIR emission spectroscopy was carried out on a Nicolet spectrophotometer equipped with a TGS detector, which was modified by replacing the IR source with an emission cell. A description of the cell and principles of the emission experiment have been published elsewhere. Approximately 0.2 mg of hydronium jarosite mineral was spread as a thin layer (approximately 0.2 microns) on a 6 mm diameter platinum surface and held in an inert atmosphere within a nitrogen-purged cell during heating.

In the normal course of events, three sets of spectra are obtained: first the black body radiation over the temperature range selected at the various temperatures, secondly the platinum plate radiation at the same temperatures and thirdly spectra from the platinum plate coated with the sample. Normally only one set of black body and platinum radiation data is required. The emittance spectrum (E) at a particular temperature was calculated by subtraction of the single beam spectrum of the platinum backplate from that of the platinum+sample, and the result ratioed to the single beam spectrum of an approximate blackbody (graphite). The following equation was used to calculate the emission spectra.

$$E = -0.5 \log \frac{Pt - S}{Pt - C}$$

This manipulation is carried out after all the data is collected. Emission spectra were collected at intervals of 50°C over the range 200–750°C. The time between scans (while the temperature was raised to the next hold point) was approximately 100 s. It was considered that this was sufficient time for the heating block and the powdered sample to reach thermal equilibrium. Spectra were acquired by 1064 scans over the temperature range 100–300°C and 128 scans over the range 350–900°C (approximate scan time 45 s), with a nominal resolution of 4 cm^{-1}. Good quality spectra can be obtained providing the sample thickness is not too large. If too large a sample is used then spectra become difficult to interpret because of the presence of combination and overtone bands. Spectroscopic manipulation such as baseline adjustment, smoothing and normalisation was performed using the GRAMS® software package (Galactic Industries Corporation, Salem, NH, USA).

Results and discussion

TG analysis and mass spectrometric analysis

The TG pattern of hydronium jarosite is shown in Fig. 1. Five mass loss steps are observed at 262, 294, 385, 557 and 619°C. The relative ion current of evolved water vapour and oxygen is shown in Fig. 2. This graph shows that water is lost almost continuously from around 250 through to 500°C. Figure 3 displays the ion current for masses of 32, 48 and 64. This graph shows the loss of sulphur dioxide and represents the loss of sulphate in the thermal decomposition process. Two temperatures are observed at 578 and 622°C. These two temperatures correspond with the mass loss steps at 557 and 619°C. There is a slight difference in the temperatures as the mass spectrometric analysis starts after the commencement of the thermal analysis. Both oxygen and SO_2 are evolved at 622°C but only SO_2 at 578°C.

The first three mass loss steps involve the evolution of water vapour and are attributed to dehydroxylation. The fourth mass loss step at 557°C involves both the loss of water and the loss of sulphate simultaneously. This mass loss step is ascribed to the loss of the hydrated proton and the loss of the associated sulphate unit. The theoretical mass loss of six hydroxyl units from hydronium jarosite based upon the formula $(H_3O)Fe_3(SO_4)_2(OH)_6$) is 21.25%. The total mass loss for the three dehydroxylation steps is 15.3%. This value is low compared with the theoretical value.

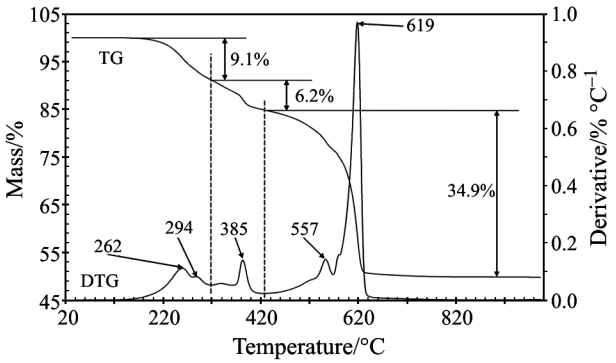

Fig. 1 Thermogravimetric and derivative thermogravimetric analysis of hydronium jarosite

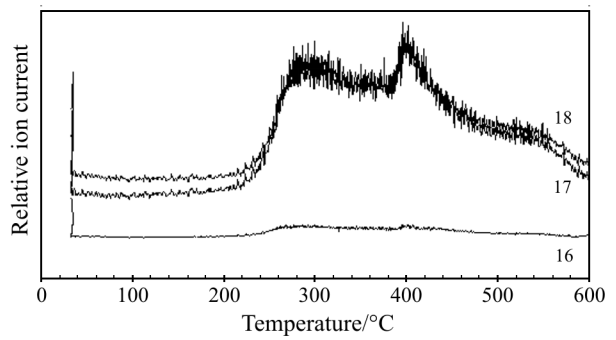

Fig. 2 Ion current curves of molar masses 16, 17 and 18 as a function of temperature

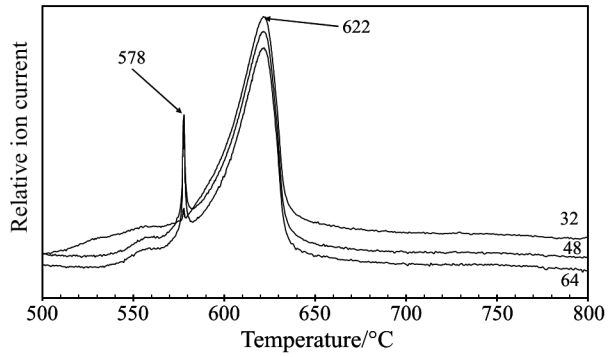

Fig. 3 Ion current curves of molar masses 32, 48 and 64 as a function of temperature

Mechanism for the thermal decomposition of hydronium jarosite

The following set of steps is proposed for the mechanism for the thermal decomposition of hydronium jarosite. Five steps are proposed. The first three steps involve the loss of hydroxyl units, the fourth step is the loss of the hydrated proton together with the loss of sulphate and the final step is due to the loss of the remaining sulphate.

Step 1 (262°C)

$$(H_3O)Fe_3(SO_4)_2(OH)_6 \rightarrow (H_3O)(Fe_3O)(SO_4)_2(OH)_4+H_2O$$

This decomposition step is due to dehydration of the hydronium jarosite

Step 2 (294 and 343°C)

$$(H_3O)(Fe_3O)(SO_4)_2(OH)_4 \rightarrow (H_3O)(Fe_3O_{1.5})(SO_4)_2(OH)_3+0.5H_2O$$

$$(H_3O)(Fe_3O_{1.5})(SO_4)_2(OH)_3 \rightarrow (H_3O)(Fe_3O_2)(SO_4)_2(OH)_2+0.5H_2O$$

This decomposition step is associated with the dehydroxylation of the hydronium jarosite.

Step 3 (at 385°C)

$$(H_3O)(Fe_3O_2)(SO_4)_2(OH)_2 \rightarrow (H_3O)(FeO)_3(SO_4)_2+H_2O$$

This step is a second dehydroxylation step.

Step 4 (at 557°C)

$$(H_3O)(FeO)_3(SO_4)_2 \rightarrow (FeO)_3(SO_4)+H_2SO_4$$

$$H_2SO_4 \rightarrow SO_3+H_2O$$

$$(FeO)_3(SO_4) \rightarrow FeSO_4+Fe_2O_3$$

$$\text{i.e. } (H_3O)(FeO)_3(SO_4)_2 \rightarrow FeSO_4+Fe_2O_3+SO_2+H_2O$$

This step is a very sharp decomposition step. This step is due to the loss of sulphate as SO_3. The step is shown in the ion current curves in Fig. 3. There is a slight lag in the mass spectrometric curves compared with the DTG curves. The sharp temperature in the DTG curves at 557°C corresponds with the temperature of 578°C for the mass gain of SO_3 and SO_2. This temperature is the temperature at which the hydrogen ion from the hydronium jarosite is lost.

Step 5 (at 619°C)

$$2FeSO_4 \rightarrow Fe_2O_3+SO_2$$

This step is the final decomposition step and is the final loss of sulphate as SO_2.

Raman and infrared spectroscopy

Materials such as hydronium jarosite may be characterised by their infrared and Raman spectra. These spectra provide an understanding of the molecular structure of the material. Changes in this structure can be followed by changes in the Raman and infrared spectra. One tech-

nique for studying the changes in the molecular structure is infrared emission spectroscopy. The technique enables the spectrum at the elevated temperature to be determined. In order to understand the spectrum at the elevated temperature it is necessary to understand the room temperature spectra. The Raman spectrum of hydronium-jarosite in the 150 to 1250 cm^{-1} range and the infrared spectrum in the infrared spectrum in the 550 to 1250 cm^{-1} range are shown in Fig. 4. Sulphates as with other oxyanions lend themselves to analysis by Raman spectroscopy. In aqueous systems, the sulphate anion is of T_d symmetry and is characterised by Raman bands at 981 cm^{-1} (ν_1), 451 cm^{-1} (ν_2), 1104 cm^{-1} (ν_3) and 613 cm^{-1} (ν_4). Reduction in symmetry in the crystal structure of sulphates such as jarosites will cause the splitting of these vibrational modes. For jarosites the space group is C_5^3 and six sulphate fundamentals should be observed. The Raman band at 1005 cm^{-1} is attributed to the SO_4^{2-} symmetric stretching mode. The equivalent infrared band is forbidden and is not observed.

In the Raman spectrum an intense sharp band is observed at 1014 cm^{-1} which is attributed to the symmetric stretching vibration of the SO_4^{2-} units. The band is only observed as a small shoulder at 1003 cm^{-1} in the infrared spectrum which is dominated by an intense band centred at 999 cm^{-1}. This band is attributed to the hydroxyl deformation modes. The Raman band corresponds well with the previously published data for synthetic jarosites [28]. Sasaki *et al.* did not publish the spectrum of hydronium jarosite. The infrared spectrum in this work differs from that published by Sasaki *et al.* for the synthetic jarosites in that the strong band at 999 cm^{-1} was not reported [28]. Two Raman bands are observed at 1171 and 1107 cm^{-1} which are assigned to the antisymmetric stretching vibrations of the SO_4^{2-} units. The position of these bands corresponds well with the published data of Sasaki *et al.* [28]. The equivalent infrared bands are observed at 1184 and 1084 cm^{-1}. Sasaki *et al.* reported infrared bands using reflectance techniques for ammonium jarosite at 1200 and 1080 cm^{-1}.

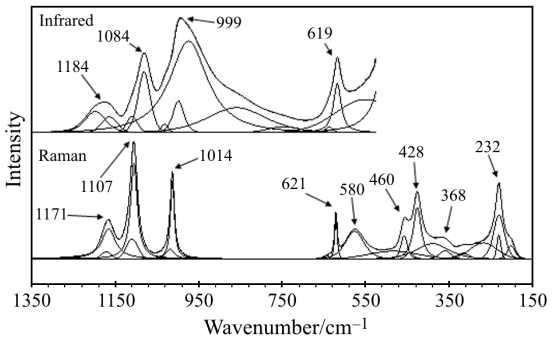

Fig. 4 Raman in the 150 to 1350 cm^{-1} region and infrared spectra in the 550 to 1350 cm^{-1} region of hydronium jarosite at 298 K

The band at 623 cm^{-1} in the infrared spectrum and at 621 cm^{-1} in the Raman spectrum is attributed to the ν_4 bending mode of the SO_4^{2-} units. It should be noted that the lower limit of the infrared spectrum is 550 cm^{-1} because of the absorption of the ATR cell. A low intensity Raman band in the Raman spectrum at 565 cm^{-1} and a band at 532 cm^{-1} may also be ascribed to this bending mode. The previous study which reported the Raman spectrum of jarosites gave for K-jarosite two infrared bands at 630 and 580 cm^{-1} and at 625 and 577 cm^{-1} in the Raman spectrum . In the Raman spectrum bands at 453 and 435 cm^{-1} are attributed to the ν_2 bending modes of the SO_4^{2-} units.

The two bands at 368 (weak) and 321 cm^{-1} are assigned to FeO stretching vibrations. Sasaki *et al.* also assigned bands in similar positions to this type of FeO vibration. These workers also assigned a band at 449 cm^{-1} as a FeO vibration. However, it is more likely that this band is due to the ν_2 bending modes of the SO_4^{2-} units. The additional band is caused by the symmetry reduction of the SO_4^{2-} units. The strong Raman band at 232 cm^{-1} is probably due to strong hydrogen bonding between the hydroxyl units and the sulphate units in the hydronium jarosite structure.

Infrared emission spectroscopy

The use of infrared emission spectroscopy enables the changes in the structure of the hydronium jarosite to be followed in situ at the elevated temperatures. No heat source is required except for the hot sample itself. As the material is heated, the infrared radiation is emitted and is detected by the infrared detector.

The infrared emission spectra of hydronium jarosite in the OH stretching region are shown in Fig. 5. This suite of spectra shows the intensity of the OH stretching units over the 100 to 400°C temperature range. No intensity remains in this band after 450°C. The conclusion is made that dehydroxylation of the hydronium jarosite is complete by this temperature.

The IE spectra of the sulphate stretching region are shown in Fig. 6. This figure shows the changes in IE spectral profile with temperature increase. These spectra have been analysed using band component analysis techniques. These resolved spectra are shown in Fig. 7. The stacked plot of the band component analyses of the 100 to 500°C IE spectra are shown in Fig. 7. In the IE spectrum at 100°C, two sets of bands are observed at 1012, 1085 and 1220 cm^{-1} and a second set at 1010, 1116 and 1184 cm^{-1}. The second set of bands are at a significantly lower intensity than the first set. In the crystal structure of jarosites there are two independent types of sulphate units in the ratio of 1:3. Infrared emission spectroscopy is identifying two sets of sulphate antisymmetric stretching vibrations which are

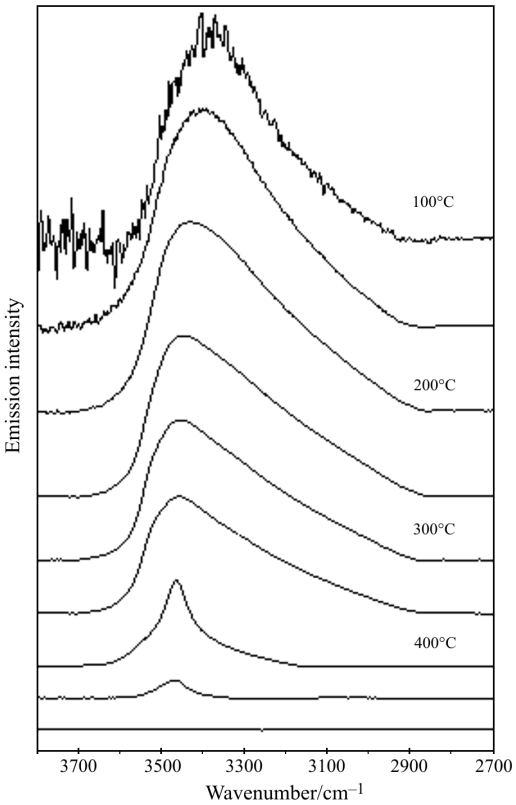

Fig. 5 Infrared emission spectra of the hydroxyl stretching region of hydronium jarosite at temperatures from 100 to 500°C, at 50°C intervals

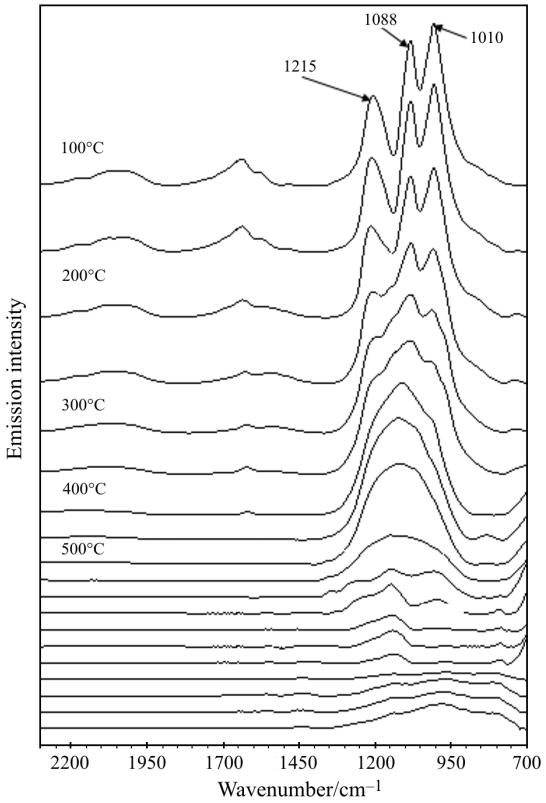

Fig. 6 Infrared emission spectra of the 700 to 2200 cm^{-1} region of hydronium jarosite at temperatures from 100 to 1000°C, at 50°C intervals

attributed to these two types of sulphate units. In the 200°C spectrum infrared emission bands are observed at 1012, 1085 and 1195 cm^{-1} with a second set of bands at 1010, 1114 and 1230 cm^{-1}. A different spectral profile is observed in the IE spectrum at 300°C. Bands are observed at 972, 1016, 1083, 1157 and 1220 cm^{-1}. Changes in the spectral profile are observed due to the onset of dehydroxylation which results in the removal of the bonding of the OH units to the sulphate units. At 400°C bands are observed at 1014, 1105 and 1220 cm^{-1} and at 500°C 1005, 1059, 1126 and 1225 cm^{-1}. The definition and resolution of the bands is lost at 550°C and no intensity remains in the spectra at 700°C. Thus this shows that the loss of sulphate has occurred by this temperature.

The changes in the IE spectra are in harmony with the thermal analysis results. Even though the two types of experiments are conducted differently. The TG experiment is a dynamic experiment with the thermal decomposition studied at a constant heating rate. The infrared emission experiment is a batch type experiment in which the hydronium jarosite is heated to a certain temperature, with a wait time of 15 min followed by collection of the data. The sample is then ramped to the next temperature and the experiment repeated.

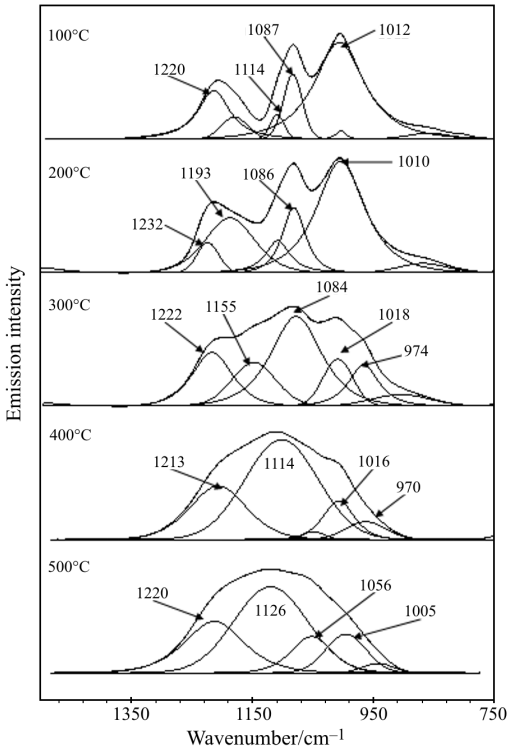

Fig. 7 Band component analysis of the 750 to 1350 cm^{-1} region of hydronium jarosite at 100 to 500°C, at 100°C intervals

Conclusions

Thermogravimetry combined with mass spectrometry has been used to study the thermal decomposition of a synthetic hydronium jarosite. The hydronium jarosite is stable up to around 200°C, after which decomposition commences and reaches a maximum at 262°C after which dehydroxylation occurs. This dehydroxylation appears to take place in steps at 262, 294, 345 and 385°C. The proton appears to be lost at 557°C and is associated with a loss of sulphate. This loss of the proton is sometimes referred to as 'excess' water. The remainder of the sulphate units are lost at 619°C. In many natural jarosites for example natrojarosite, the mineral is not purely a sodium jarosite but may contain some protons and thus one is dealing with a mixed sodium–hydronium jarosite. Changes in the molecular structure were followed using infrared emission spectroscopy.

Jarosites are a group of minerals formed in evaporite deposits and form a component of efflorescence. As such the minerals can function as cation and heavy metal collectors. Hydronium jarosite has the potential to act as a cation collector by replacement of the proton with a heavy metal cation. The potential of this synthetic mineral for this purpose remains to be explored.

Acknowledgements

The financial and infra-structure support of the Queensland University of Technology Inorganic Materials Research Program of the School of Physical and Chemical Sciences is gratefully acknowledged.

The Australian Research Council (ARC) is thanked for funding.

References

1 J. Kubisz, Bull. Acad. Polon. Sci., Ser. Sci., Chim., Geol. Geograph., 8 (1960) 95.
2 J. Kubisz, Przeglad Geologiczny, 17 (1969) 583.
3 J. A. Ripmeester, C. I. Ratcliffe, J. E. Dutrizac and J. L. Jambor, Canadian Mineralogist, 24 (1986) 435.
4 D. Karamanev, J. Biotechnol., 20 (1991) 51.
5 K. Koiwasaki, Y. Honbou, K. Tazaki and T. Mori, Chikyu Kagaku (Chigaku Dantai Kenkyukai), 47 (1993) 493.
6 T. Buckby, S. Black, M. L. Coleman and M. E. Hodson, Mineralogical Magazine, 67 (2003) 263.
7 P. A. Williams, Oxide Zone Geochemistry, Ellis Horwood Ltd., Chichester, West Sussex, England 1990.
8 S. Nagai and N. Yamanouchi, Nippon Kagaku Kaishi 1921–47, 52 (1949) 83.
9 J. L. Kulp and H. H. Adler, Am. J. Sci., 248 (1950) 475.
10 G. Cocco, Periodico di Mineralogia, 21 (1952) 103.
11 A. I. Tsvetkov and E. P. Val'yashikhina, Doklady Akademii Nauk SSSR, 89 (1953) 1079.
12 A. I. Tsvetkov and E. P. Val'yashikhina, Doklady Akademii Nauk SSSR, 93 (1953) 343.
13 V. P. Ivanova, Zapiski Vserossiiskogo Mineralogicheskogo Obshchestva, 90 (1961) 50.
14 M. Hartman, V. Vesely and K. Jakubec, Collection of Czechoslovak Chemical Communications, 52 (1987) 939.
15 M. S. R. Swamy, T. P. Prasad and B. R. Sant, J. Thermal Anal., 16 (1979) 471.
16 M. S. R. Swamy, T. P. Prasad and B. R. Sant, J. Thermal Anal., 15 (1979) 307.
17 S. Bhattacharyya and S. N. Bhattacharyya, J. Chem. Eng. Data, 24 (1979) 93.
18 M. S. R. Swami and T. P. Prasad, J. Thermal Anal., 19 (1980) 297.
19 M. S. R. Swamy and T. P. Prasad, J. Thermal Anal., 20 (1981) 107.
20 A. C. Banerjee and S. Sood, Therm. Anal., Proc. Int. Conf., 1 (1982) 769.
21 J. E. Dutrizac and J. L. Jambor, Chapter 8 Jarosites and their application in hydrometallurgy , (2000) 405.
22 R. L. Frost and K. L. Erickson, J. Therm. Anal. Cal., 76 (2004) 217.
23 R. L. Frost, K. Erickson and M. Weier, J. Therm. Anal. Cal., 77 (2004) 851.
24 R. L. Frost, M. L. Weier and K. L. Erickson, J. Therm. Anal. Cal., 76 (2004) 1025.
25 R. L. Frost and M. L. Weier, J. Therm. Anal. Cal., 75 (2004) 277.
26 R. L. Frost, W. Martens, Z. Ding and J. T. Kloprogge, J. Therm. Anal. Cal., 71 (2003) 429.
27 R. L. Frost, Z. Ding and H. D. Ruan, J. Therm. Anal. Cal., 71 (2003) 783.
28 K. Sasaki, O. Tanaike and H. Konno, Canadian Mineralogist, 36 (1998) 1225.

Received: January 14, 2005
In revised form: May 25, 2005

DOI: 10.1007/s10973-005-6908-0